Do Porous Titanium Granule Grafts Affect Bone Microarchitecture at Augmented Maxillary Sinus Sites? A Pilot Split-Mouth Human Study

Erhan Dursun, DDS, PhD,* Ceyda Kanli Dursun, DDS, PhD,† Kenan Eratalay, DDS, PhD,‡ Kaan Orhan, DDS, PhD,§ Hakan Hamdi Celik, MD,¶ and Tolga Fikret Tözüm, DDS, PhD||

Background: *The aim of this randomized controlled clinical study was to analyze the bone microarchitecture at augmented maxillary sinus sites by using different materials in patients to compare the effect of porous titanium granules as a sinus augmentation material with bone microstructural features.*

Materials and Methods: *Eight subjects with bilateral atrophic posterior maxilla of residual bone height <4 mm included in this study and each patient was treated with bilateral sinus augmentation procedure using xenograft with equine origin (Apatos, Osteobiol; Tecnoss Dental) and xenograft (1 g) + porous titanium (1 g) granules (Natix; Tigran Technologies AB). Sixteen human bone biopsy samples were taken from patients receiving two-stage sinus augmentation therapy during implant installation and analyzed using microcomputerized tomography. Three-dimensional bone structural parameters were analyzed in details: tissue volume, bone volume, percentage of bone volume, bone surface and bone surface density, bone specific surface, trabecular thickness trabecular separation, trabecular number, trabecular pattern factor, structural model index, fractal dimension, and bone mineral density.*

Results: *No statistically significant differences were found between groups according to bone structural parameters.*

Conclusions: *Porous titanium grafts may ensure a space for new bone formation in the granules, which may be a clinical advantage for long-term success. (Implant Dent 2015;0:1–7)*

Key Words: sinus, bone substitute, microtomography, human, dental implant

Although many techniques allow clinicians to treat more complex cases, the success of dental implant procedure is dependent on many factors, which include patient-originated and procedure-dependent variables. The quality of the bone and the type of surgical procedure are primary factors for long-term survival of dental implants.[1–3]

Gender, genetics, systemic conditions, tooth loss sequence, length of edentulous time, and other unknown factors influence the chronic remodeling/resorption process of jaws and affecting the quality of bone for potential implant sites.[4–7] Maxillary sinus lifting/augmentation is a routine procedure for improving prognosis of implants placement in maxillary posterior area, which is well described and an accepted procedure in the literature.[8,9]

*Assistant Professor, Department of Periodontology, Faculty of Dentistry, Hacettepe University, Ankara, Turkey.
†Private Practice in Periodontics, Ankara, Turkey.
‡Professor, Department of Periodontology, Faculty of Dentistry, Hacettepe University, Ankara, Turkey.
§Professor, Department of Dentomaxillofacial Radiology, Faculty of Dentistry, Ankara University, Ankara, Turkey.
¶Professor, Department of Anatomy, Faculty of Medicine, Hacettepe University, Ankara, Turkey.
||Associate Professor, Department of Periodontics, College of Dentistry, University of Illinois at Chicago, Chicago, IL.

Reprint requests and correspondence to: Tolga Fikret Tözüm, DDS, PhD, Department of Periodontics, College of Dentistry, University of Illinois at Chicago, 801 South Paulina Street Room 469G, Chicago, IL 60612, Phone: 312-996-0265, Fax: 312-996-0943, E-mail: ttozum@uic.edu

ISSN 1056-6163/15/00000-001
Implant Dentistry
Volume 0 • Number 0

DOI: 10.1097/ID.0000000000000274

There are numerous studies in the literature on the use of autogenous bone grafts since it was first demonstrated in 1980.[9–11] Autogenous bone provides satisfactory results with osteoinductive properties.[8,12] However, the volume of bone at the donor site that can be harvested is limited, which requires a second donor site surgery and thus potential morbidity for the patient. It has been also reported that significant resorption of the autologous bone graft may occur over time, which may compromise long-term implant stability.[13,14] Alternatively, natural or synthetic materials have been used successfully for maxillary sinus augmentation. Although many studies evaluated the favorability of materials of different origins, it still remains unclear, which is

the most suitable grafting material for maxillary sinus augmentation.[12,13,15–18]

Porous titanium granules (PTG) (Natix; Tigran Technologies AB, Malmö, Sweden) are novel grafting materials with 700 to 1000 μm diameter and have a pore size above 50 μm in diameter. The porous properties may lead to ingrowth of newly formed bone.[19] The granules have been tested in orthopedic surgery for fixation of femoral stems, and histology from both clinical and experimental studies have shown bone formation in and around the titanium granules.[20] In a recent study, Verket et al[14] reported successful results with PTG when used as a single grafting material for sinus augmentation.

Another challenge for the clinicians in this area is that the posterior maxilla has a poorer bone quality with the highest percentage of type 4 bone. Therefore, bone structural evaluation of possible dental implant site together with maxillary sinus augmentation procedure in this area is crucial for successful treatment. Structural changes that occur during the healing of graft materials have been described and analyzed by means of histomorphometric analysis. Although this kind of evaluation provides valuable information, it is still 2-dimensional (2D) information for a 3-dimensional (3D) material.[2,15,18,21]

Moreover, it should be indicated that whether in the bone or in the graft material, the resorption occurs in a 3D and nonuniform pattern. Thus, 3D evaluation of morphological changes is an important tool in the analysis.[10] Various 3D evaluations can be used in evaluation of bone and bone grafts in dental implant sites such as computerized tomography (CT),[3] quantitative CT,[2,22] and recently, cone-beam CT.[23]

Micro-CT offers innovative and noninvasive techniques that allow the study of the processes occurring within human hard tissues, without the need to destroy the specimen.[24] By doing so, micro-CT makes it possible for the use of same specimens for several different biological and mechanical tests.[25,26] A recent development in 3D imaging of cancellous bone has made possible true 3D quantification of trabecular architecture. Analysis such as bone volume fraction, trabecular thickness, trabecular separation, trabecular number, trabecular bone pattern factor, structural model index (SMI) can be performed using micro-CT scanning.[21,25,26] These measurements are important because the trabecular structure of bone is a 3D nature, which correlates with mechanical and biological properties.[21,26] The micro-CT method has been used as a technique to evaluate the ridge augmentation both qualitatively and quantitatively.[2] Although, there is an increase demand in the studies with micro-CT for evaluating the grafts, still only very limited studies were conducted for comparison between different graft materials by means of 3D structural changes.[8,14,16,21,23,27]

Hence, it was considered worthwhile to analyze the bone microarchitecture at augmented maxillary sinus sites and to in-patient evaluate the effect of PTG as a sinus augmentation material to bone microstructural features using micro-CT in a human randomized controlled study.

MATERIALS AND METHODS

Patient Selection Criteria

Eight patients were included in the study (5 men and 3 women, mean age = 48.14 ± 9.16 years), and each patient was treated with bilateral sinus augmentation procedure using equine derived xenograft (Apatos, Osteobiol; Tecnoss Dental, Turin, Italy) and xenograft (1 g) + porous titanium (1 g) granules. Selection of which side (right or left) will receive test or control biomaterial inside each sinus lift was done by a randomization process (coin toss). Inclusion criteria were bilateral maxillary edentulism involving the premolar/molar regions and the presence of <4 mm bone between maxillary sinus floor and alveolar crest. The patients having systemic problems that would jeopardize the bone healing process (metabolic and/or bone diseases, uncontrolled diabetes), severe parafunctional habits, drug or alcohol abuse, smoking, poor oral hygiene, and untreated periodontal disease were excluded from the study. Preoperative panoramic x-rays and dental volumetric CT images were obtained. Every patient was treated with two-stage sinus augmentation surgery. According to two-stage surgical approach, after 6 months of healing, bone biopsies were retrieved from 16 implant sites with a trephine bur with 2 mm internal diameter and 3 mm external diameter during the implant insertion by crestal approach (Fig. 1).

Micro-CT Scanning

A high resolution, micro-CT system (Skyscan 1174; Skyscan, Kontich, Belgium) was used to scan the specimen. Before scanning, the specimen were rinsed and stored in saline solution (0.9%) within a sterile tube. The scanning conditions were 50 kVp, 100 mA beam current, 0.5 mm Al filter, 17.3 μm pixel size, rotation at 0.5 step, three-frame averaging beam hardening 40%. To minimize ring artifacts, air calibration of the detector was performed before each scanning. Each sample was rotated 360 degree within an integration time of 5 minutes. Mean time of scanning was around 2 hours. Other settings included beam hardening correction, as already described above, and input of optimal contrast limits (0–0.0006) based on previous scanning and reconstruction of the specimen.

Micro-CT Image Analysis

NRecon software (Skyscan 1174; Skyscan) was used for visualization and quantitative measurements of the samples, which used the modified algorithm described by Feldkamp et al[28] to obtain axial 2D, 1000 × 1000-pixel images (Fig. 2). For the reconstruction

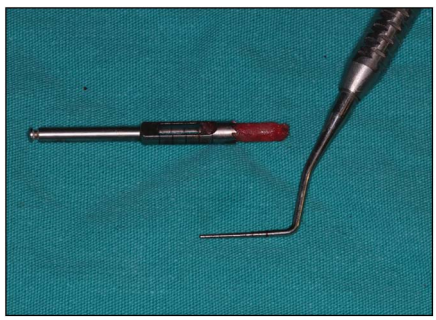

Fig. 1. According to two-stage surgical approach, after 6 months of healing, bone biopsies were retrieved from 16 implant sites with a trephine bur with 2 mm internal diameter and 3 mm external diameter during the implant insertion by crestal approach.

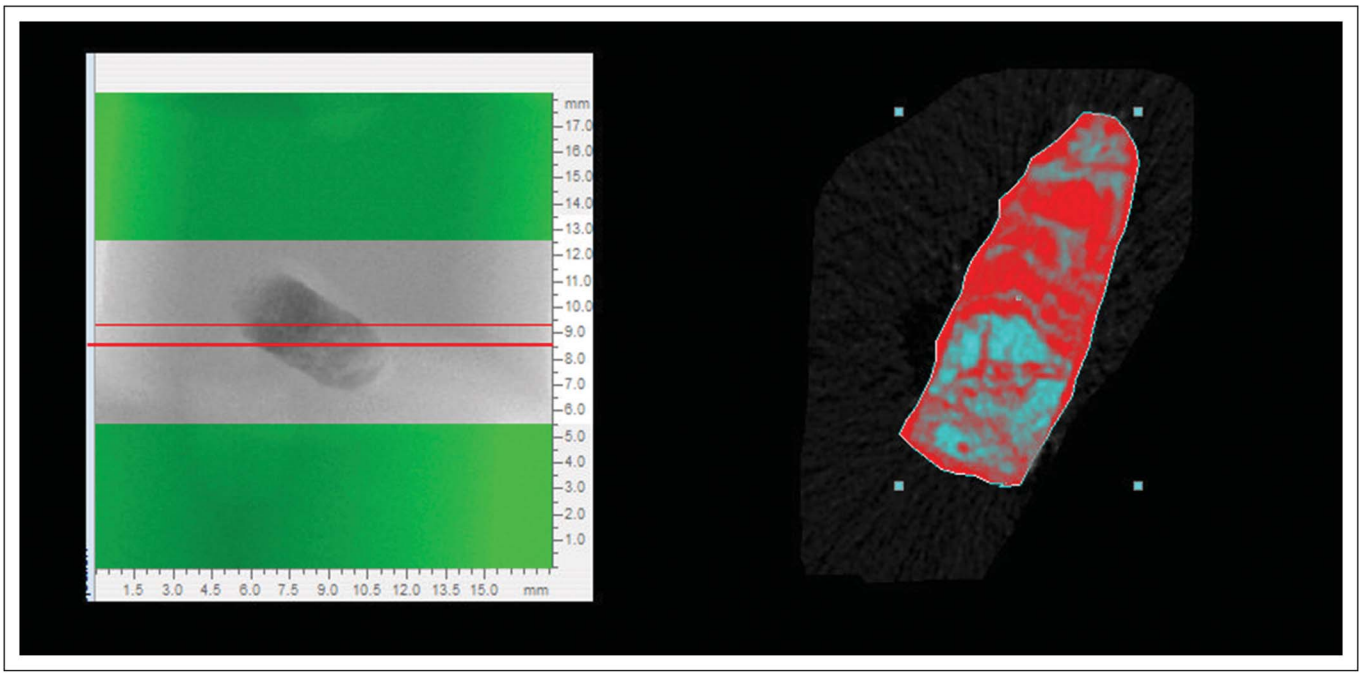

Fig. 2. NRecon software was used for visualization and quantitative measurements of the samples to obtain axial 2D, 1000 × 1000–pixel images.

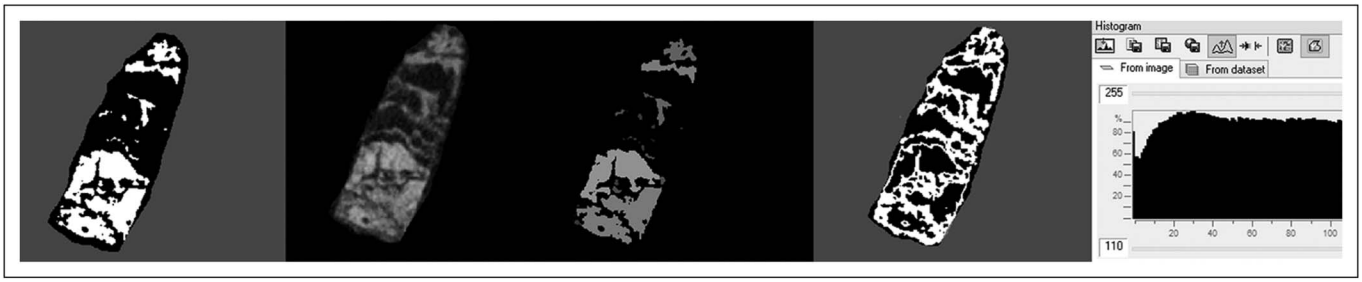

Fig. 3. The reconstructed micro-CT images showing threshold of the sample was used to distinguish from native and grafted bone (threshold set to 110–255).

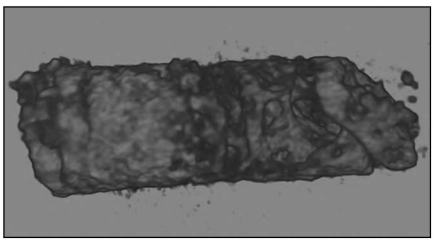

Fig. 4. A representative image of the micro-CT 3D reconstruction of a bone biopsy sample. It demonstrates the regions of native and grafted bone.

parameters, ring artifact correction and smoothing were fixed at zero and the beam artifact correct later set at 40%. Contrast limits were applied according to manufacturer instructions. A similar

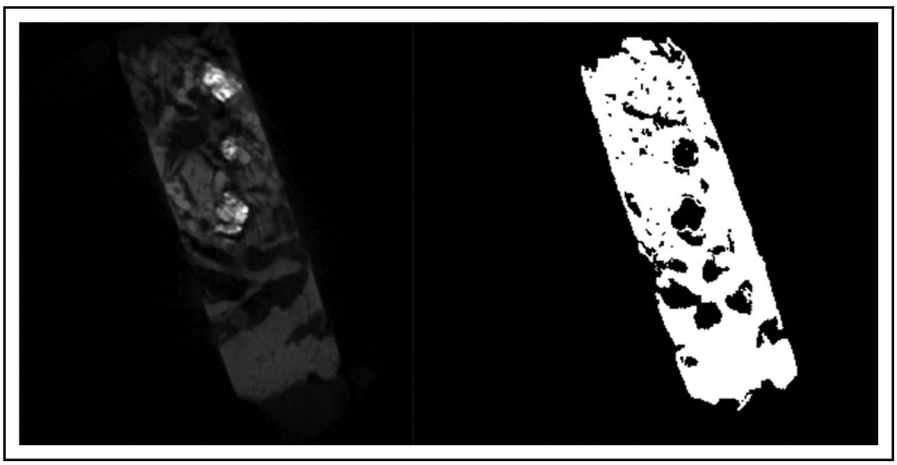

Fig. 5. Bone biopsy sample before and after thresholding. Threshold was set as the lower limit was between 110 and 255 (in gray values), and the upper limit was at the top end of the brightness spectrum representing the highest bone density value.

Table 1. Bone Structural Parameters of All Specimens According to CT Scan Software

Patient No.	Sex	TV (mm^3)	BV (mm^3)	BV/TV (%)	BS (mm^2)	BS/BV (mm^{-1})	BS/TV (mm^{-1})	Tb.Pf (mm^{-1})	Tb.Th (mm)	Tb.Sp (mm)	Tb.N (mm^{-1})	SMI	FD	BMD
T1	M	2.87	1.004	34.9	59.99	59.7	20.95	–68.48	0.33	0.62	1.04	1.1	1.869	358.05
C1	M	1.09	2.85	26	41.56	14.55	38.12	–44.51	0.3	0.66	1.61	2.5	2.62	385.64
T2	F	3.61	4.83	13.33	90.1	18.64	25.02	–81.83	0.36	0.77	1.2	2.32	2.38	434.96
C2	F	5.4	2.66	20.3	90.6	33.9	16.6	–80.7	0.22	0.89	2.06	2.8	2.68	424.19
C3	M	5.5	3.22	58.3	25.37	7.87	4.24	–90	0.92	0.57	1.014	1.93	1.95	701.15
T3	M	6.5	3	47	26.6	8.67	4.07	–14	0.63	0.61	1.13	2.6	2.8	607.35
C4	F	4.11	2.95	71.8	95.3	32.2	23.1	–34.7	0.11	0.15	6.4	1.4	2.45	317.82
T4	F	4.65	3.15	14.7	14.9	4.7	3.01	–17.5	0.15	0.28	8.12	1.5	2.15	399.72
T5	M	4.8	2.27	21	36.9	16.2	7.55	–43.6	0.51	0.13	4.2	0.93	2.78	499.15
C5	M	12.76	7.69	36	45.6	5.29	3.57	–44.4	0.37	0.18	4.3	1.2	1.85	498.16
T6	M	6.29	2.49	25.2	71.6	28.71	11.3	–78.2	0.29	0.89	1.191	1.6	1.78	525.16
C6	M	8.63	5.12	16.8	55.8	11.08	6.46	–80.6	0.43	0.21	3.84	2.9	1.85	434.58
T7	F	3.6	3.17	11	29.6	9.33	8.22	–39.7	0.37	0.2	0.3	1.3	2.67	424.50
C7	F	28	12.55	40	49.9	39.81	1.75	–31.1	0.08	0.14	0.5	2.8	2.23	400.66
T8	M	12.54	4.76	26	49.9	10.4	3.98	–3.32	0.08	0.22	0.3	2.7	2.23	610.23
C8	M	3.79	2.35	46	59.6	16	25.36	–93.6	0.38	0.11	0.75	234	3.37	555.16

BMD indicates bone mineral density; BS/BV, bone specific surface; BS/TV, bone surface density; BV/TV, percent bone volume; C, control group; CPB, closed porosity of bone; T, test group; Tb.N, trabecular number; Tb.Pf, trabecular pattern factor; Tb.Sp, trabecular separation; Tb.Th, trabecular thickness.

Table 2. Statistical Analysis of Bone Structural Parameters Between Groups

Bone Structural Parameters	Test (Mean ± SD)	Control (Mean ± SD)	*P*
TV (mm^3)	5.6 ± 3.08	8.66 ± 8.56	0.484
BV (mm^3)	3.08 ± 1.26	4.92 ± 3.55	0.263
BV/TV (%)	24.14 ± 12.13	39.4 ± 18.96	0.069
BS (mm^2)	47.44 ± 25.32	57.96 ± 23.95	0.484
BS/BV (mm^{-1})	19.54 ± 17.86	20.08 ± 13.21	0.889
BS/TV (mm^{-1})	10.51 ± 8.23	14.9 ± 13.11	0.575
Tb.Pf (mm^{-1})	–43.32 ± 30.4	–62.45 ± 26.16	0.401
Tb.Th (mm)	0.34 ± 0.17	0.35 ± 0.26	0.944
Tb.Sp (mm)	0.46 ± 0.29	0.36 ± 0.29	0.293
Tb.N (mm^{-1})	2.18 ± 2.69	2.55 ± 2.08	0.208
SMI	–14.71 ± 8.42	–18.73 ± 11.7	0.401
FD	2.33 ± 0.39	2.37 ± 0.52	0.889
BMD	482.39 ± 54.06	464.67 ± 56.80	0.760

BS/BV indicates bone-specific surface; BS/TV, bone surface density; BV/TV, percent bone volume; C, control group; CPB, closed porosity of bone; T, test group; Tb.N, trabecular number; Tb.Pf, trabecular pattern factor; Tb. Sp, trabecular separation; Tb.Th, trabecular thickness.

procedure was used to measure gray values of 2 bone mineral density (BMD) phantom rods. To aid BMD calculations; grayscale values were converted to BMD values (in $gHAp \cdot cm^{-3}$) with a linear calibration curve based on the grayscale values obtained from the 2 different mineral concentration conical phantoms of 0.25 and 0.75 $gHAp \cdot cm^{-3}$. Calculation of mineral loss difference (ΔZ; $gHAp \cdot cm^{-3}$) was made by subtracting BMD values of each group from baseline BMD values.

After reconstruction, region of interests were drawn within the sample (Fig. 3) using CT scan, in which all specifications of the program was used to analyze the 3D microarchitecture of each sample (Fig. 4). To distinguish grafted bone from original bone from the background, which consists of saline solution, a suitable threshold is required. Therefore, threshold was set as follows: the lower limit was between 110 and 255 (in gray values) and the upper limit was at the top end of the brightness spectrum representing the highest bone density value (Fig. 5). Ten structural parameters in each bone sample were measured over the entire volume of the specimen in line with Monje et al[29] and similar studies[26,30–34] as:

1. Tissue volume (TV), bone volume (BV), percent bone volume (BV/TV): BV/TV refers to the total amount of bone present in relation to the analyzed BV. It is a parameter widely used in pathologies that alter bone turnover as it reflects perfectly bone gain/loss. It indicates the fraction of a given volume of interest occupied by mineralized tissue.
2. Bone surface (BS) of the sample and bone surface density (BS/BV) is the relationship between the overall trabecular BS and the BV of mineralized bone.
3. Bone specific surface (BS/TV) analyzes the relation between the trabecular BS and the mineralized bone. In a 3D image, it directly measures distance in space.
4. Trabecular thickness determines bone fill and the mean thickness of the osseous structures.
5. Trabecular separation (Tb.Sp) detects marrow spaces and thus it should be correlated to BV/TV: the more BV/TV, the less Tb.Sp. This parameter determines inverse bone density.

6. Trabecular number implies the number of times a trabecular structure is crossed per unit length in a randomly selected way.
7. Bone quality is determined by direct nonmetric parameters. Trabecular pattern factor (Tb.Pf) describes quantitatively trabecular connectivity. It is an inverse connectivity index. Therefore, concavity of the trabecular surfaces implies connectivity, whereas convexity means isolated and misconnected structures.
8. SMI determines the relative presence of either plate-like or rod-like trabeculae. It is defined in a range of 0 to 3, where closer to 0 corresponds to and ideal plate and 3 to an ideal cylinder. Plate-like trabecula is associated with a higher osseous stiffness.
9. Fractal dimension (FD): fractal analysis is a statistical texture analysis that is based on fractal mathematics for describing complex shapes and structural patterns. It is expressed numerically as "fractal dimension" (FD), which measures self-similarity and indicates a figure's complexity.
10. BMD compares between the attenuation coefficients of 2 hydroxyapatite patterns of known density (250 and 750 mg/cm^3). This is a density of the area not a true volume density as it has a dependency on bone size.

Statistical Analysis

All of the micro-CT measurement parameters are summarized as median values and interquartile ranges (25th percentile [Q1]–75th percentile [Q3]). The parameters between the groups were compared with Wilcoxon rank-sum test. The correlations among the parameters were calculated using Spearman rank correlation coefficient.

RESULTS

A total of 16 sinus augmentation surgeries were performed, and Table 1 summarizes the bone microstructural values of 16 bone samples that were retrieved from 8 patients and Table 2 details the significant differences between groups. No significant differences were found between groups according to bone structural parameters including BMD. In both groups, no significant correlations were found between BMD and any other bone structural parameters. When all patients were analyzed, significant correlations were found between BV/TV and Tb.Th as well as Tb.N and BS/BV. Significant correlations were found in test group according to Tb.Th (mm) and mean FD ($r = -0.786$, $P = 0.021$), Tb.Pf (mm^{-1}) and BS/TV (mm^{-1}) ($r = -0.881$, $P = 0.004$), SMI and BS/TV (mm^{-1}) ($r = 0.714$, $P = 0.047$), BS/TV (mm^{-1}) and BS/BV (mm^{-1}) ($r = 0.81$, $P = 0.015$), and BS (mm^2) and Tb.Pf (mm^{-1}) ($r = -0.738$, $P = 0.037$).

DISCUSSION

According to the literature, maxillary sinus grafting is a routine procedure for improving prognosis of implant placement in maxillary posterior area which is well described and an accepted procedure in the literature.[8,9] Successful results have been reported with different grafting materials such as autografts, xenografts, alloplastic materials, and with combination of these materials.[35–38] Beside the insufficient bone height, maxillary posterior area usually composed by type 3 to type 4 bone due to the porous thin layer of cortical bone and fine trabecular bone.[39] Trabecular bone plays a significant role in bone strength and determines its biomechanical properties.[40] Cortical and trabecular bone structures are important determinants of bone quality and associated long-term implant success.[40]

X-ray examination is a routine method to assess the grafted bone situation after sinus augmentation. Although the x-ray–based technique is noninvasive, it provides only low-resolution 2D images.[8] Histology and histomorphometric techniques can be used to examine the bone mineral quality and trabecular bone structure of grafted bone, but they can only provide one-time measurements that cannot be repeated on the same sample.[41] Moreover, only both x-rays can obtain a few sections, and histomorphometric methods and these 2D images may not be representative of the entire specimen.[8] Micro-CT has been reported as a highly precision method for the analysis of bone and biomaterials.[42] This study was conducted to evaluate the bone microstructure at augmented maxillary sinus sites with different graft materials by micro-CT. The quality and quantity of the residual native bone in the posterior maxilla may influence the microarchitecture of the grafted bone and may be a confounding factor.[29] However, no significant differences according to residual bone height and the in-patient study design may overcome this limitation. This approach may shed light to morphologic and structural changes after sinus augmentation.

Comparing BMD and other bone structural parameters in grafted bone and/or different bone types may ensure better understanding of remodeling phases of the bone grafts and may help to predict the success of future dental implant treatment.[8] In this study, no significant correlations were found between BMD and other parameters. Our findings are not in accordance with Huang et al,[8] where they reported significant correlations with BMD and BV/TV and Tb.N at autogenously grafted maxillary sinus. This inconsistency may be due to the difference between osteoinductive and osteoconductive properties of different grafting materials. Significant correlations between BV/TV and Tb.Th as well as Tb.N and BS/BV in the grafted maxillary sinus are in accordance with Huang et al and may be suggested that the size and the number of the grafted bone trabeculae are dependent to the volume of bone structure.

Huang et al[8] reported the 3D bone structure and BMD analysis findings, where they used autogenous graft for sinus augmentation and compared the grafted bone with native bone. They reported significant differences between autogenously grafted bone and native bone according to surface complexity, trabecular thickness, and trabecular separation.[8] Chappard et al[42] used β-tricalcium phosphate (β-TCP) for

sinus augmentation and analyzed bone samples by micro-CT and suggested β-TCP as a suitable sinus augmentation material. According to this study, no significant differences were detected between 2 grafting materials according to bone microstructure parameters suggested that both grafting materials may function as an augmentation material. This study and studies of this kind may ensure better understanding of remodeling and mineralization phases of bone healing after sinus lifting surgery and may give information about the bone quality at the posterior maxilla after sinus augmentation.

Conclusions

This clinical pilot study was concluded with PTG as sinus augmentation material showed no significant improvements when mixed with xenograft according to bone microstructural parameters. However, its porosity ensures a space for new bone formation in the granules, which may be a clinical advantage for long-term success. Analyzing the augmented bone microarchitecture by micro-CT, which allows 3D visualization of the bone sample, may be a useful tool to understand the mechanisms underlying bone healing process. Further studies are necessary to develop standard numeric values in 3D evaluations for bone structural parameters that may be useful to predict long-term success of augmentation procedures and associated implant procedures.

Disclosures

The authors claim to have no financial interest, either directly or indirectly, in the products or information listed in the article.

Acknowledgments

This study is supported by Hacettepe University, Scientific Research Projects Coordination Unit (Grant Number: 011D10201003), Ankara, Turkey.

Approval

The study was approved by the Institutional Review Board of Hacettepe University (Approval number: HEK 11/70-2).

References

1. Ekfeldt A, Christiansson U, Eriksson T, et al. A retrospective analysis of factors associated with multiple implant failures in maxillae. *Clin Oral Implants Res.* 2001; 12:462–467.

2. Kim YJ, Henkin J. Micro-computed tomography assessment of human alveolar bone: Bone density and three-dimensional micro-architecture. *Clin Implant Dent Relat Res.* 2015;17:307–313.

3. Ozan O, Orhan K, Turkyilmaz I. Correlation between bone density and angular deviation of implants placed using CT-generated surgical guides. *J Craniofac Surg.* 2011;22:1755–1761.

4. Carlsson GE. Responses of jawbone to pressure. *Gerodontology*. 2004; 21:65–70.

5. Klemetti E. A review of residual ridge resorption and bone density. *J Prosthetic Dent.* 1996;75:512–514.

6. Pietrokovski J, Kaffe I, Arensburg B. Retromolar ridge in edentulous patients: Clinical considerations. *J Prosthodont.* 2007;16:502–506.

7. Xie Q, Ainamo A, Tilvis R. Association of residual ridge resorption with systemic factors in home-living elderly subjects. *Acta Odontol Scandinav.* 1997; 55:299–305.

8. Huang HL, Chen MY, Hsu JT, et al. Three-dimensional bone structure and bone mineral density evaluations of autogenous bone graft after sinus augmentation: A microcomputed tomography analysis. *Clin Oral Implants Res.* 2012;23:1098–1103.

9. Boyne PJ, James RA. Grafting of the maxillary sinus floor with autogenous marrow and bone. *J Oral Surg.* 1980;38: 613–616.

10. Deluiz D, Oliveira LS, Pires FR, et al. Time-dependent changes in fresh-frozen bone block grafts: Tomographic, histologic, and histomorphometric findings. *Clin Implant Dent Relat Res.* 2015; 17:296–306.

11. Misch CM. Maxillary autogenous bone grafting. *Oral Maxillofac Surg Clin North Am.* 2011;23:229–238.

12. Caubet J, Petzold C, Saez-Torres C, et al. Sinus graft with safescraper: 5-Year results. *J Oral Maxillofac Surg.* 2011;69: 482–490.

13. Schlegel KA, Fichtner G, Schultze-Mosgau S, et al. Histologic findings in sinus augmentation with autogenous bone chips versus a bovine bone substitute. *Int J Oral Maxillofac Implants.* 2003; 18:53–58.

14. Verket A, Lyngstadaas SP, Rasmusson L, et al. Maxillary sinus augmentation with porous titanium granules: A microcomputed tomography and histologic evaluation of human biopsy specimens. *Int J Oral Maxillofac Implants.* 2013;28:721–728.

15. Miyamoto S, Shinmyouzu K, Miyamoto I, et al. Histomorphometric and immunohistochemical analysis of human maxillary sinus-floor augmentation using porous beta-tricalcium phosphate for dental implant treatment. *Clin Oral Implants Res.* 2013;24(suppl A100): 134–138.

16. Kuhl S, Gotz H, Brochhausen C, et al. The influence of substitute materials on bone density after maxillary sinus augmentation: A microcomputed tomography study. *Int J Oral Maxillofac Implants.* 2012; 27:1541–1546.

17. Butz F, Bachle M, Ofer M, et al. Sinus augmentation with bovine hydroxyapatite/synthetic peptide in a sodium hyaluronate carrier (PepGen P-15 Putty): A clinical investigation of different healing times. *Int J Oral Maxillofac Implants.* 2011;26: 1317–1323.

18. Boeck-Neto RJ, Gabrielli M, Lia R, et al. Histomorphometrical analysis of bone formed after maxillary sinus floor augmentation by grafting with a combination of autogenous bone and demineralized freeze-dried bone allograft or hydroxyapatite. *J Periodontol.* 2002;73: 266–270.

19. Bystedt H, Rasmusson L. Porous titanium granules used as osteoconductive material for sinus floor augmentation: A clinical pilot study. *Clin Implant Dent Relat Res.* 2009;11:101–105.

20. Turner TM, Urban RM, Hall DJ, et al. Bone in growth through porous titanium granulate around a femoral stem: Histological assessment in a six-month canine hemiarthroplasty model. *Upsal J Med Sci.* 2007;112:191–197.

21. Villanueva-Alcojol L, Monje F, Gonzalez-Garcia R, et al. Characteristics of newly formed bone in sockets augmented with cancellous porous bovine bone and a resorbable membrane: Microcomputed tomography, histologic, and resonance frequence analysis. *Implant Dent.* 2013;22:380–387.

22. Homolka P, Beer A, Birkfellner W, et al. Bone mineral density measurement with dental quantitative CT prior to dental implant placement in cadaver mandibles: Pilot study. *Radiology*. 2002;224: 247–252.

23. Soardi CM, Zaffe D, Motroni A, et al. Quantitative comparison of cone beam computed tomography and microradiography in the evaluation of bone density after maxillary sinus augmentation: A

Preliminary study. *Clin Implant Dent Relat Res.* 2014;16:557–564.

24. Davis GR, Wong FS. X-ray microtomography of bones and teeth. *Physiologic Measure.* 1996;17:121–146.

25. Swain MV, Xue J. State of the art of Micro-CT applications in dental research. *Int J Oral Sci.* 2009;1:177–188.

26. Hildebrand T, Ruegsegger P. Quantification of bone microarchitecture with the structure model Index. *Comput Met Biomec Biomed Eng.* 1997;1:15–23.

27. Rebaudi A, Trisi P, Cella R, et al. Preoperative evaluation of bone quality and bone density using a novel CT/microCT-based hard-normal-soft classification system. *Int J Oral Maxillofac Implants.* 2010;25:75–85.

28. Feldkamp LA, Goldstein SA, Parfitt AM, et al. The direct examination of three-dimensional bone architecture in vitro by computed tomography. *J Bone Mineral Res.* 1989;4:3–11.

29. Monje A, Monje F, Gonzalez-Garcia R, et al. Influence of atrophic posterior maxilla ridge height on bone density and microarchitecture. *Clin Implant Dent Relat Res.* 2015;17:111–119.

30. Parfitt AM. Bone histomorphometry: Proposed system for standardization of nomenclature, symbols, and units. *Calcif Tissue Int.* 1988;42:284–286.

31. Hahn M, Vogel M, Pompesius-Kempa M, et al. Trabecular bone pattern factor—A new parameter for simple quantification of bone microarchitecture. *Bone*. 1992;13:327–330.

32. Odgaard A, Gundersen HJ. Quantification of connectivity in cancellous bone, with special emphasis on 3-D reconstructions. *Bone*. 1993;14:173–182.

33. Tosoni GM, Lurie AG, Cowan AE, et al. Pixel intensity and fractal analyses: Detecting osteoporosis in perimenopausal and postmenopausal women by using digital panoramic images. *Oral Surg Oral Med Oral Pathol Oral Radiol Endod.* 2006;102:235–241.

34. Southard TE, Southard KA, Krizan KE, et al. Mandibular bone density and fractal dimension in rabbits with induced osteoporosis. *Oral Surg Oral Med Oral Pathol Oral Radiol Endod.* 2000;89:244–249.

35. Ramirez-Fernandez MP, Calvo-Guirado JL, Mate-Sanchez Del Val JE, et al. Ultrastructural study by backscattered electron imaging and elemental microanalysis of bone-to-biomaterial interface and mineral degradation of porcine xenografts used in maxillary sinus floor elevation. *Clin Oral Implants Res.* 2013;24:523–530.

36. Ramirez-Fernandez MP, Calvo-Guirado JL, Delgado-Ruiz RA, et al. Ultrastructural study by backscattered electron imaging and elemental microanalysis of biomaterial-to-bone interface and mineral degradation of bovine xenografts in maxillary sinus floor elevation. *Clin Oral Implants Res.* 2013;24:645–651.

37. Barone A, Ricci M, Covani U, et al. Maxillary sinus augmentation using prehydrated corticocancellous porcine bone: Histomorphometric evaluation after 6 months. *Clin Implant Dent Relat Res.* 2012;14:373–379.

38. Orsini G, Scarano A, Piattelli M, et al. Histologic and ultrastructural analysis of regenerated bone in maxillary sinus augmentation using a porcine bone-derived biomaterial. *J Periodontol.* 2006;77:1984–1990.

39. Misch CE. Bone classification, training keys to implant success. *Dent Today.* 1989;8:39–44.

40. Carballido-Gamio J, Majumdar S. Clinical utility of microarchitecture measurements of trabecular bone. *Curr Osteoporos Rep.* 2006;4:64–70.

41. Gedrange T, Hietschold V, Mai R, et al. An evaluation of resonance frequency analysis for the determination of the primary stability of orthodontic palatal implants. A study in human cadavers. *Clin Oral Implants Research.* 2005;16:425–431.

42. Chappard D, Guillaume B, Mallet R, et al. Sinus lift augmentation and beta-TCP: A microCT and histologic analysis on human bone biopsies. *Micron*. 2010;41:321–326.